

# A terpyridyl-imidazole (tpy-HImzPh<sub>3</sub>) based bifunctional receptor for multichannel detection of Fe<sup>2+</sup> and F<sup>-</sup> ions†

Chanchal Bhaumik, Shyamal Das, Dinesh Maity and Sujoy Baitalik\*

Received 24th May 2011, Accepted 18th August 2011

DOI: 10.1039/c1dt10965k

The X-ray crystal structures of the tridentate ligand, 4'-[4-(4,5-diphenyl-1*H*-imidazol-2-yl)-phenyl]-[2,2':6',2'']terpyridine (tpy-HImzPh<sub>3</sub>) and its bis-homoleptic iron(II) complex of composition [Fe(tpy-HImzPh<sub>3</sub>)<sub>2</sub>]<sup>2+</sup> have been determined, showing that the ligand crystallized in a monoclinic form with the space group *P*2<sub>1</sub>/*c* while its Fe(II) complex crystallizes in an orthorhombic form with space group *F*ddd. Both the anion and cation binding properties of the receptor were thoroughly investigated in dimethylformamide-acetonitrile (1 : 9) solution using absorption, emission, and <sup>1</sup>H NMR spectral studies which revealed that the receptor acts as a sensor for both F<sup>-</sup> and Fe<sup>2+</sup>. In the presence of excess F<sup>-</sup> ion, deprotonation of the imidazole N–H fragment of the receptor occurs, an event which is signaled by the development of a yellow color visible with the naked eye. The estimated value of the equilibrium constant of the receptor with F<sup>-</sup> is 1.9 × 10<sup>4</sup> M<sup>-1</sup>. Deprotonation is also observed in the presence of hydroxide. The receptor also shows colorimetric and fluorimetric sensing ability towards Fe<sup>2+</sup> ions. The binding site for the metal ion in the system has been unambiguously established by single-crystal X-ray diffraction studies of the Fe(II) complex of the receptor. The influence of solvents on the absorption and fluorescence spectra of the receptor has been investigated in detail. Cyclic voltammetric (CV) and square wave voltammetric (SWV) measurements carried out in dimethylformamide-acetonitrile (2 : 3) provided evidence in favor of cation (Fe<sup>2+</sup>) and anion (F<sup>-</sup>) concentration dependent electrochemical responses, enabling the ligand to act as a suitable electrochemical sensor for F<sup>-</sup> and Fe<sup>2+</sup> ions.

## Introduction

The design of sensors capable of recognizing and sensing both cations and anions is one of the most challenging fields because of the important role they play in biological, industrial and environmental processes.<sup>1–11,15–21</sup> The sensitive and selective detection of ferrous and fluoride ions is important because of their crucial biological roles. Among the transition metals, iron is the most important element involved in living systems.<sup>12–15</sup> Biologically, iron plays crucial roles in the transport and storage of oxygen and also in electron transport in diverse metalloenzymes.<sup>12–15</sup> Iron is truly ubiquitous in living systems and tracking its homeostasis using a suitable technique is of great significance to clarify its biological effects.<sup>22</sup> On the other hand, fluoride plays an important role in preventing dental caries and in the treatment of osteoporosis.<sup>1–5,16</sup> High doses of this anion are, however, dangerous and can lead to dental or skeletal fluorosis.<sup>16</sup> This diversity of function makes the

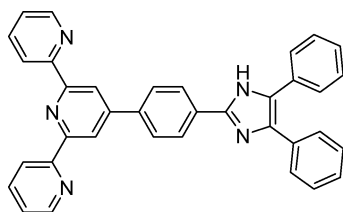
problem of iron and fluoride ion detection one of considerable current interest. Consequently, much effort has been directed towards the design of receptors that can selectively recognize either anions or cations.<sup>1–11</sup> A number of compounds containing urea, thiourea, amide, pyrrole or imidazole subunits that are capable of providing hydrogen bond forming sites have been reported to exhibit strong affinity and selectivity towards certain anions.<sup>1–11</sup> On the other hand, different types of ligands with N, O, or S donor centers act as binding sites for several transition metal cations.<sup>12–22</sup> The majority of these chemosensors are three-component systems comprising a signaling unit, a guest binding unit, and a linker that connects these two units.<sup>5–10</sup> Although a number of chemosensors have been developed for the detection of transition metal cations and anions,<sup>15–29</sup> sensing of both Fe<sup>2+</sup> and F<sup>-</sup> ions by a single receptor is still rather rare.

In recent years, the development of triple channel sensors, that is sensors where interactions can be sensed by monitoring three different physicochemical outputs (absorption, emission and redox properties), have emerged as a topic of considerable interest.<sup>30,31</sup> To this end, in our search for appropriate ligands for the construction of suitable multichannel sensors that are capable of recognizing cations and anions, we have found that the 4'-[4-(4,5-diphenyl-1*H*-imidazol-2-yl)-phenyl]-[2,2':6',2'']terpyridine<sup>32</sup> (tpy-HImzPh<sub>3</sub>) system, wherein a terpyridine moiety has been fused at its 4'-position with the 2,4,5 triphenyl imidazole motif, has yet

Department of Chemistry, Inorganic Chemistry Section, Jadavpur University, Kolkata, 700 032, India. E-mail: sbaitalik@hotmail.com; Fax: + 91 3324146584; Tel: + 91 33 24146666

† Electronic supplementary information (ESI) available: Fig. S1–S14, Table S1–S3 and X-ray crystallographic file in CIF format for the free receptor and its Fe(II) complex. CCDC reference numbers 817562–817563. For ESI and crystallographic data in CIF or other electronic format see DOI: 10.1039/c1dt10965k

to be exploited in the area of sensor development. Tridendate ligands, such as terpyridine (tpy), are known to form complexes with a large variety of transition metal ions.<sup>33</sup> Moreover, these binding moieties are versatile building blocks in supramolecular and macromolecular chemistry.<sup>33–36</sup> In contrast to the related 2,2'-bipyridine (bpy) ligand, which gives rise to the formation of  $M(\text{bpy})_3^{2+}$ -type metal complexes with  $\Delta/\Lambda$  chirality, tpy forms achiral octahedral coordination compounds of the type  $M(\text{tpy})_2^{2+}$ .<sup>34</sup> In order to accomplish our goal, we have exploited the fluoride ion signaling potential of the imidazole NH group and transition metal ion binding ability of the terpyridine moiety. To our knowledge, no such studies have been reported in literature for multichannel detection of both  $\text{Fe}^{2+}$  and  $\text{F}^-$  ions using a terpyridyl-imidazole type of ligand. As will be seen, as a consequence of cation/anion interaction, remarkable changes in color (that can be followed by the naked eye) along with similar absorption, photoluminescence and redox responses occur.



**Tpy-HImzPh<sub>3</sub>**

## Experimental

### Materials

Reagent grade chemicals obtained from commercial sources were used as received. Solvents were purified and dried according to standard methods.<sup>37</sup> Benzil and tetrabutylammonium (TBA) salt of the anions were purchased from Sigma-Aldrich. 4'-(*p*-methylphenyl)-2,2':6',2''-terpyridine (**tpy-PhCH<sub>3</sub>**), 4'-(*p*-dibromomethylphenyl)-2,2':6',2''-terpyridine (**tpy-PhCHBr<sub>2</sub>**), 4'-formyl-2,2':6',2''-terpyridine (**tpy-PhCHO**), were synthesized according to the literature procedures.<sup>31d,38–41</sup>

**Preparation of the ligand 4'-[4-(4,5-diphenyl-1H-imidazol-2-yl)phenyl]-[2,2':6',2''] terpyridine (tpy-HImzPh<sub>3</sub>).** The synthesis of the compound was undertaken by following a method previously described.<sup>32</sup> A mixture of 4'-(*p*-formylphenyl)-2,2':6',2''-terpyridine (tpy-PhCHO) (1.00 g, 2.97 mmol), benzil (630 mg, 3.00 mmol), and ammonium acetate (2.3 g, 30 mmol) in acetic acid (30 mL) was heated at reflux for 2 h. The resulting orange-red solution was cooled to room temperature and poured into crushed ice (250 mL) with vigorous stirring. A grey colored precipitate thus obtained was filtered off. It was then slurried with water (*ca.* 200 mL) and slowly treated with 25% aqueous ammonia to pH  $\approx$  8 when the color changed to light pink. The solid was collected by filtration and washed several times with water. The residue was purified by silica gel column chromatography in chloroform and recrystallized from chloroform-methanol (1 : 1) to give the desired compound as a light green crystalline solid (1.41 g, 2.68 mmol, yield 87%). <sup>1</sup>H NMR (DMSO, 300 MHz):  $\delta$  = 12.90 (s, 1H, NH(imidazole)), 8.78 (m, 4H (2H3'+2H6)), 8.68 (d, 2H,  $J$  = 7.9 Hz, H3), 8.30 (d, 2H,  $J$  = 8.0 Hz, H8), 8.09–8.00 (m, 4H (2H4 + 2H7)), 7.58–7.20 (m, 12H (10H (phenyl) + 2H5)). ESI-MS:  $m/z$

527.63 ([L+H]<sup>+</sup>). Anal. Calcd for C<sub>36</sub>H<sub>25</sub>N<sub>5</sub>: C, 81.95; H, 4.78; N, 13.27. Found: C, 81.87; H, 4.81; N, 13.25.

**Synthesis of [Fe(tpy-HImzPh<sub>3</sub>)<sub>2</sub>](ClO<sub>4</sub>)<sub>2</sub>.** To a stirred chloroform-methanol (1 : 1) solution (30 mL) of the ligand (0.11 g, 0.21 mmol) was added solid Fe(ClO<sub>4</sub>)<sub>2</sub>·6H<sub>2</sub>O (0.36 g, 0.1 mmol). The colorless solution changed immediately to violet, and during stirring at room temperature for  $\sim$ 1 h a microcrystalline compound deposited. The compound was filtered, washed with water, and dried in a vacuum. On recrystallization from acetonitrile-methanol (1 : 1) a violet crystalline compound was obtained: yield 0.10 g (76%). <sup>1</sup>H NMR (DMSO, 300 MHz):  $\delta$  = 13.02 (s, 2H, NH(imidazole)), 9.73 (s, 4H, H3'), 9.08 (d, 4H,  $J$  = 8.0 Hz, H3), 8.70 (d, 4H,  $J$  = 8.4 Hz, H8), 8.50 (d, 4H,  $J$  = 8.3 Hz, H7), 8.04 (t, 4H,  $J$  = 7.6 Hz, H4), 7.63–7.29 (m, 24H (20 phenyl-H + 4H6)), 7.20 (t, 4H,  $J$  = 6.4 Hz, H5). Anal. Calcd for C<sub>72</sub>H<sub>50</sub>N<sub>10</sub>Cl<sub>2</sub>O<sub>8</sub>Fe: C, 66.00; H, 3.84; N, 10.69. Found: C, 65.95; H, 3.81; N, 10.71. ESI-MS (positive, CH<sub>3</sub>CN)  $m/z$  = 554.75 (100%) [Fe(tpy-HImzPh<sub>3</sub>)<sub>2</sub>]<sup>2+</sup>; 1209.12 (5%) [Fe(tpy-HImzPh<sub>3</sub>)<sub>2</sub>(ClO<sub>4</sub>)<sub>2</sub>]<sup>+</sup>.

**Caution!** Perchlorate salts of different metals and of the Fe(II) complex used in this study are potentially explosive and therefore should be handled in small quantities with care.

### Physical measurements

Elemental (C, H, and N) analyses were performed on a Perkin-Elmer 2400II analyzer. Electrospray ionization mass spectra (ESI-MS) were obtained on a Micromass Qtof YA 263 mass spectrometer. <sup>1</sup>H and {<sup>1</sup>H–<sup>1</sup>H} COSY spectra were obtained on a Bruker Avance DPX 300 spectrometer using DMSO-*d*<sub>6</sub> solutions. Electronic absorption spectra were obtained with a Shimadzu UV 1800 spectrophotometer at room temperature. The sensing studies of the receptor with different anions and cations were carried out in dimethylformamide-acetonitrile (1 : 9) solution. For a typical titration experiment, 2  $\mu$ L aliquots of a given cation or anion ( $2.0 \times 10^{-2}$  M) were added to a 2.5 mL solution of the ligand ( $2.0 \times 10^{-5}$  M). TBA salts of different anions and hydrated perchlorate salts of the metals were used for titration experiments. The binding/equilibrium constants of the anions were evaluated from the absorbance data using eqn (1).<sup>42</sup>

$$A_{\text{obs}} = (A_0 + A_{\infty}K[G]_{\text{T}})/(1 + K[G]_{\text{T}}) \quad (1)$$

where  $A_{\text{obs}}$  is the observed absorbance,  $A_0$  is the absorbance of the free receptor,  $A_{\infty}$  is the maximum absorbance induced by the presence of a given anionic guest,  $[G]_{\text{T}}$  is the total concentration of the guest, and  $K$  is the binding constant of the host–guest entity. Binding constants were performed in duplicate, and the average value is reported.

Emission spectra were recorded on a Perkin-Elmer LS55 fluorescence spectrophotometer. Photoluminescence titrations were carried out with the same sets of solutions as were made for spectrophotometry. Quantum yields of the free receptor and its Zn(II) complexes were determined in different solvents by a relative method using quinine sulfate for the free receptor and [Ru(bipy)<sub>3</sub>]<sup>2+</sup> for the Zn(II) complexes as the standard.<sup>43</sup> Time-correlated single photon counting (TCSPC) measurements were carried out for the luminescence decay of the ligand in different solvents at room temperature. For TCSPC measurement, the photoexcitation was performed at 300 nm for the free receptor and at 370 nm for the Zn(II) complexes using a picosecond diode laser (IBH

Nanoled-07) in an IBH Fluorocube apparatus. The fluorescence decay data were collected on a Hamamatsu MCP photomultiplier (R3809) and were analyzed using IBH DAS6 software.

The electrochemical measurements were carried out with a BAS 100B electrochemistry system. A three-electrode assembly comprising a Pt (for oxidation) or glassy carbon (for reduction) working electrode, Pt auxiliary electrode, and an aqueous Ag/AgCl reference electrode was used. The cyclic voltammetric (CV) and square wave voltammetric (SWV) measurements were carried out at 25 °C in dimethylformamide-acetonitrile (2 : 3) solution of the complexes (*ca.* 1 mM) and the concentration of the supporting electrolyte tetraethylammonium perchlorate (TEAP) was maintained at 0.1 M. All of the potentials reported in this study were referenced against the Ag/AgCl electrode, which under the given experimental conditions gave a value of 0.36 V for the ferrocene/ferrocenium couple. For electrochemical titrations 25  $\mu$ L aliquots of a perchlorate salt of a cation and TBA salts of the anions ( $4.0 \times 10^{-2}$  M in acetonitrile) were added to a 5 mL ( $1.0 \times 10^{-3}$  M) solution of the ligand.

Experimental uncertainties were as follows: absorption maxima,  $\pm 2$  nm; molar absorption coefficients, 10%; emission maxima,  $\pm 5$  nm; excited-state lifetimes, 10%; luminescence quantum yields, 20%; redox potentials,  $\pm 10$  mV.

### X-ray crystal structure determination

Diffraction quality crystals of the ligand were obtained by slow evaporation of a chloroform-ethanol (3 : 2) solution, whereas for the iron complex they were formed by diffusing toluene into a dichloromethane-acetonitrile (2 : 1) solution. X-ray diffraction data for the crystals mounted on a glass fiber and coated with perfluoropolyether oil were collected on a Bruker-AXS SMART APEX II diffractometer at room temperature equipped with CCD detector using graphite-monochromated Mo-K $\alpha$  radiation ( $\lambda = 0.71073$  Å). Crystallographic data and details of structure determination are summarized in Table 1. The data were processed with SAINT<sup>44</sup> and absorption corrections were made with SADABS.<sup>44</sup> The structure was solved by direct and Fourier methods and refined by full-matrix least-square based on  $F^2$  using the WINGX software which utilizes SHELX-97.<sup>45</sup> For structure solution and refinement the SHELXTL software package<sup>46</sup> was used. The nonhydrogen atoms were refined anisotropically, while the hydrogen atoms were placed with fixed thermal parameters at idealized positions. The electron density map showed the presence of some unassignable peaks, which were removed by running the program SQUEEZE.<sup>47</sup>

The final least-squares refinement ( $I > 200\sigma(I)$ ) converged to reasonably good  $R$  values (Table 1).

## Results and discussion

### Synthesis and characterization

A mixture of benzil and 4'-(*p*-formylphenyl)-2,2':6',2''-terpyridine (tpy-PhCHO) in a 1 : 1 molar ratio was subjected to undergo condensation in acetic acid in the presence of excess of ammonium acetate for the synthesis of the ligand, tpy-HImzPh<sub>3</sub>. When a methanol-chloroform solution of the ligand (2 equivalents) was treated with Fe(ClO<sub>4</sub>)<sub>2</sub> (1 equivalent) the solution became intensely

**Table 1** Crystallographic data for the receptor tpy-HImzPh<sub>3</sub> and the Fe(II) complex [Fe(tpy-HImzPh<sub>3</sub>)<sub>2</sub>]<sup>2+</sup>

Compounds	Tpy-HImzPh <sub>3</sub>	[Fe(tpy-HImzPh <sub>3</sub> ) <sub>2</sub> ] <sup>2+</sup>
Formula	C <sub>36</sub> H <sub>25</sub> N <sub>5</sub>	C <sub>72</sub> H <sub>50</sub> N <sub>10</sub> Cl <sub>2</sub> O <sub>8</sub> Fe
fw	527.61	1309.97
$T$ (K)	273(2)	296(2)
Cryst. Syst.	Monoclinic	Orthorhombic
Space group	$P2_1/c$	Fddd
$a$ (Å)	14.6483(15)	23.5948(16)
$b$ (Å)	18.3958(19)	36.253(3)
$c$ (Å)	10.1403(11)	38.053(3)
$\alpha$ (°)	90	90
$\beta$ (°)	93.376(7)	90
$\gamma$ (°)	90	90
$V$ (Å <sup>3</sup> )	2727.7(5)	32 550(4)
Dc (g cm <sup>-3</sup> )	1.285	1.069
Z	4	16
$\mu$ (mm <sup>-1</sup> )	0.077	0.303
$F(000)$	1104	10 816
$\theta$ range (deg)	1.78–25.11	1.55–25.20
data/restraints/params	4830/0/370	7307/0/420
GOF on $F^2$	0.909	0.990
$R_1$ [ $I > 2\sigma(I)$ ]	0.0491	0.0664
$wR_2$ (all data)	0.1617	0.2247
$\Delta\rho_{\max}/\Delta\rho_{\min}$ (e Å <sup>-3</sup> )	0.187/−0.214	0.800/−0.377

$$^a R_1(F) = [\sum \|F_0 - |F_c|\| / \sum |F_0|], \quad ^b wR_2(F^2) = [\sum w(F_0^2 - F_c^2)^2 / \sum w(F_0^2)]^{1/2}$$

violet and the complex was isolated from the solution as a dark violet crystalline solid. Both the ligand and its Fe(II) complex have been characterized by elemental (C, H and N) analyses, ESI-MS, UV-Vis and <sup>1</sup>H NMR spectroscopic measurements and the results are given in the Experimental section. The ESI-MS of the Fe(II) complex in CH<sub>3</sub>CN (Fig. S1(b), ESI†) shows two abundant peaks at  $m/z$  554.75 and 1209.12, respectively. The isotopic patterns of the original peak at  $m/z$  554.75 separated by 0.5 Da fit very well to the isotope distribution pattern calculated for [Fe(tpy-HImzPh<sub>3</sub>)<sub>2</sub>]<sup>2+</sup> (100%). The peak at  $m/z$  1209.12 is assigned to [Fe(tpy-HImzPh<sub>3</sub>)<sub>2</sub>(ClO<sub>4</sub>)]<sup>+</sup> (5%).

### Description of crystal structures of tpy-HImzPh<sub>3</sub> and [Fe(tpy-HImzPh<sub>3</sub>)<sub>2</sub>]<sup>2+</sup>

The terpyridyl-imidazole ligand crystallized in a monoclinic form with the space group  $P2_1/c$  while its Fe(II) complex [Fe(tpy-HImzPh<sub>3</sub>)<sub>2</sub>]<sup>2+</sup> crystallizes in an orthorhombic form with space group Fddd. Structural projections of the ligand and its Fe(II) complex are shown in Fig. 1. Selected bond distances and angles of the Fe(II) complex are given in Table 2, while for the receptor are listed in Table S1 and S2, ESI.†

The X-ray crystal structure of the ligand showed that the three pyridine rings of the terpyridine moiety adopt a *transoid* arrangement about the interannular C–C bonds, which is in agreement with the literature.<sup>48</sup> This configuration minimizes electrostatic interactions between the nitrogen lone pairs and the van der Waals interactions between the *meta* protons. The interannular C–C bond length [1.488(3) Å] is comparable with those of the reported 2,2':6',2'' terpyridine derivatives [1.480(1)–1.498(3) Å].<sup>22,48</sup> The C–C and C–N bond lengths in the pyridyl and phenyl rings, in the range 1.357(4)–1.492(3) and 1.328(3)–1.346(3) Å, lie within the expected ranges. The dihedral angles between the central pyridine plane and the two lateral ones are

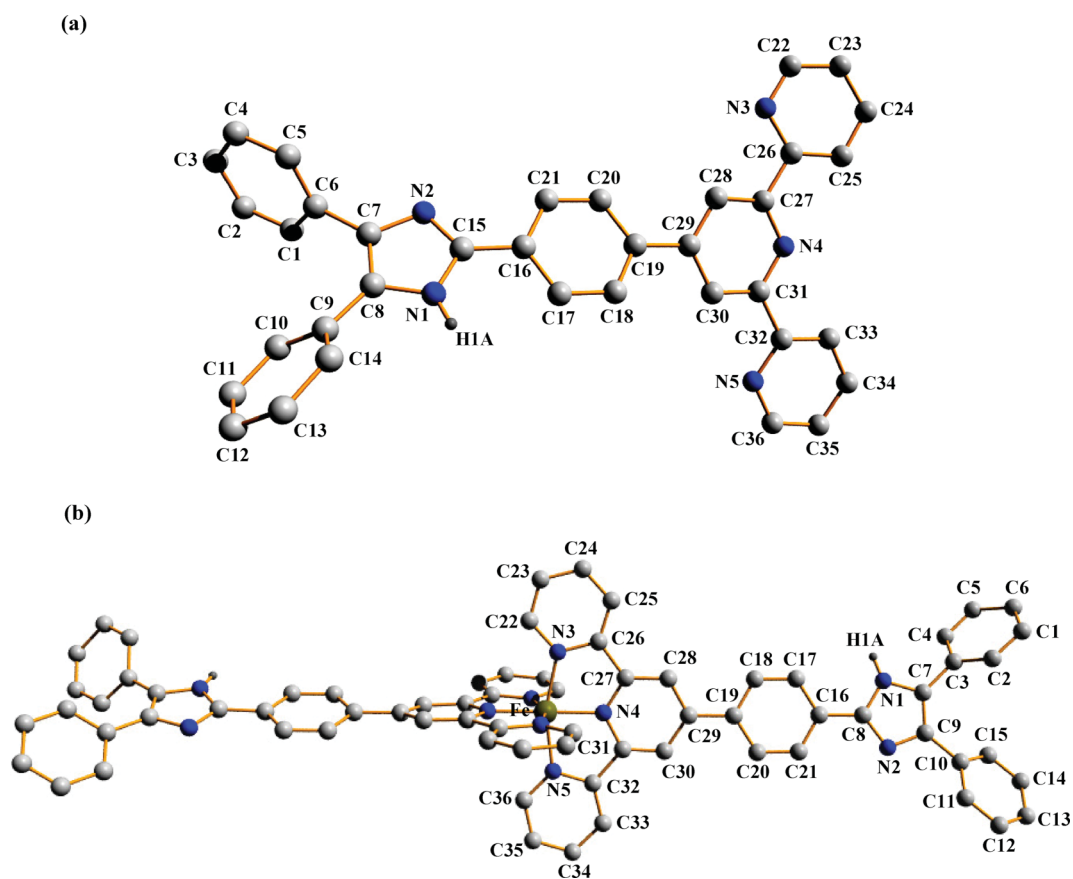


**Fig. 1** Structural projections of the receptor tpy-HImzPh<sub>3</sub> (a) and the complex cation [Fe(tpy-HImzPh<sub>3</sub>)<sub>2</sub>]<sup>2+</sup> (b). Hydrogen atoms except imidazole N–H (H1A) are omitted for clarity.

**Table 2** Selected bond distances (Å) and angles (deg) for [Fe(tpy-HImzPh<sub>3</sub>)<sub>2</sub>]<sup>2+</sup>

[Fe(tpy-HImzPh <sub>3</sub> ) <sub>2</sub> ] <sup>2+</sup>	
Fe–N(3)	1.968(3)
Fe–N(4)	1.877(2)
Fe–N(5)	1.977(3)
N(3)–Fe–N(3)	89.26(15)
N(4)–Fe–N(3)	80.52(10)
N(4)–Fe–N(3)	99.60(10)
N(5)–Fe–N(3)	92.82(10)
N(5)–Fe–N(3)	161.59(10)
N(4)–Fe–N(4)	179.83(15)
N(5)–Fe–N(4)	81.09(11)
N(5)–Fe–N(4)	98.79(10)
N(5)–Fe–N(5)	90.96(14)

10.98 and 16.44°, while the dihedral angle between the phenyl group attached to the central pyridine and imidazole moiety is 14.42°. Again the two phenyl groups are twisted heavily from the plane of the imidazole ring and the dihedral angles are 42.75 and 66.54°.

In the structure of the ligand, it is interesting to note that the NH proton of the imidazole ring is involved in strong intermolecular hydrogen bonding interactions with the N atom of a neighboring ligand, with an N–H···N distance of 2.172 Å, forming infinite chains (Fig. 2). The N–H proton of tpy-HImzPh<sub>3</sub> could be used

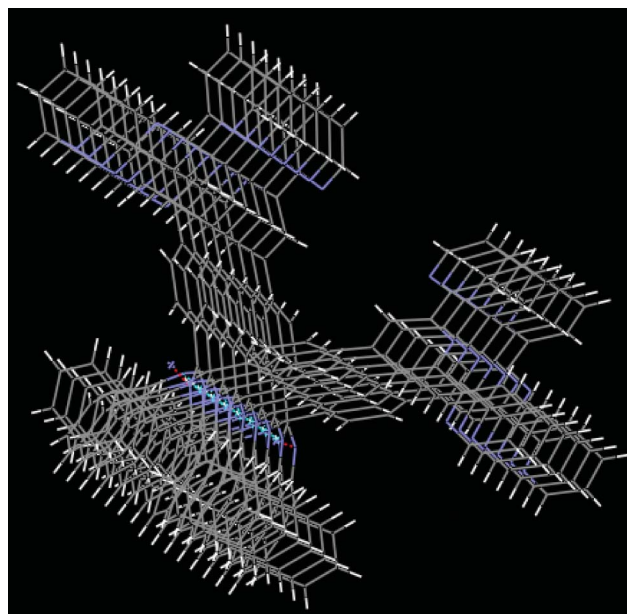


**Fig. 2** Capped-stick projection of the receptor showing intermolecular hydrogen bonding interactions.

for the formation of adducts with the anions *via* hydrogen bonding interactions.

The structure of the complex cation  $[\text{Fe}(\text{tpy-HImzPh}_3)_2]^{2+}$ , which has crystallographically imposed symmetry, is shown in Fig. 1(b). In the bis-chelated complex, the bivalent iron is coordinated by the tridentate ligand and has a distorted octahedral geometry having a meridional  $\text{N}_3\text{N}_3$  chromophore. The chelate bite angles span the range between  $80.5$  and  $99.6^\circ$ . It is to be noted that although the inter-ligand *trans* angle made by  $\text{N4-Fe-N4}$  is  $179.83^\circ$ , very close to linearity, the intra-ligand *trans* angle,  $\text{N3-Fe-N5}$ , is  $161.59^\circ$  and deviates largely from linearity. The central Fe–N bond,  $1.877(2)$  Å, is shorter than the two outer bonds of  $1.968(3)$  and  $1.977(3)$  Å to each ligand, probably because of efficient overlap of the metal  $t_{2g}$  orbital with the  $\pi^*$  orbitals of the central pyridyl group. Similar to that of the free receptor, each phenyl ring in the Fe(II) complex is also twisted with respect to the plane of the imidazole group (the corresponding dihedral angles are  $17.80$  and  $52.60^\circ$  respectively).

### $^1\text{H}$ NMR spectra

The  $^1\text{H}$  NMR spectra of both the receptor and  $[\text{Fe}(\text{tpy-HImzPh}_3)_2](\text{ClO}_4)_2$  complex recorded in  $\text{DMSO-}d_6$  (Fig. 3) show the occurrence of a number of resonances in the aromatic region. The COSY spectra have been particularly useful to locate spin couplings of these protons. The numbering scheme used to assign the observed resonances is given in Fig. 3. The distinct signal, which is the most downfield-shifted, is observed as a singlet at  $12.90$  ppm for the ligand and  $13.02$  ppm for its Fe(II) complex and is due to the imidazole NH proton. The protons of two phenyl rings attached to the imidazole moiety are characterized by a

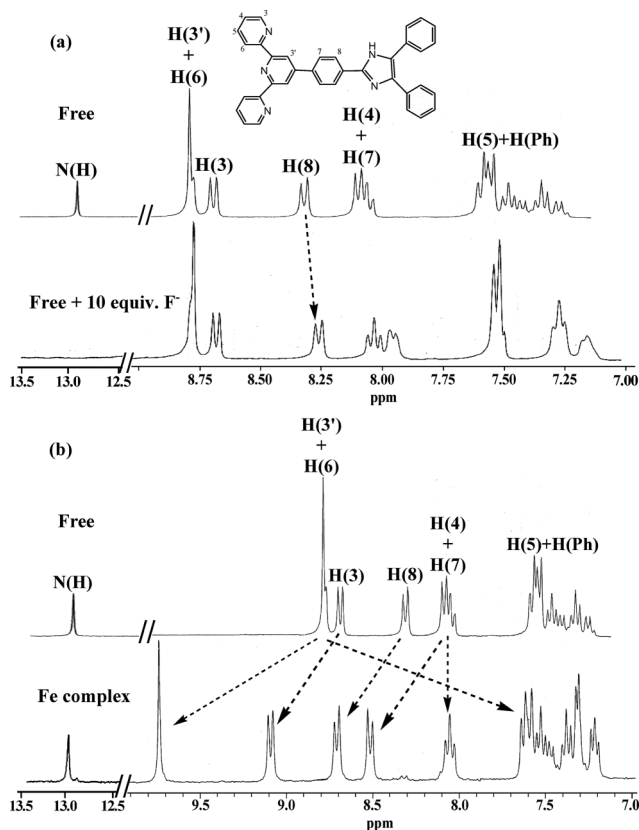


**Fig. 3**  $^1\text{H}$  spectra of the receptor in the absence and presence of (a) 10 equiv.  $\text{F}^-$  and (b) 0.5 equiv.  $\text{Fe}(\text{ClO}_4)_2$  in  $\text{DMSO-}d_6$ .

group of signals in the region  $7.20$ – $7.58$  ppm, assigned on the basis of coupling constants and chemical shifts. The terpyridine protons H3–H6, on the other hand, lie in the range  $7.20$ – $8.78$  ppm. Fig. 3(a) shows that addition of  $\text{F}^-$  leads to complete removal of the N–H signal and small upfield shifts of H8 and phenyl ring protons, although the chemical shifts for the tpy protons are far less affected. Clearly, the  $\text{F}^-$  ion acts as a proton abstractor. The upfield shift of C–H8 and protons of two phenyl rings in the ligand is due to augmentation of electron density at these sites due to delocalization of the negative charge of the imidazole ring brought about by N–H deprotonation.

The  $^1\text{H}$  NMR spectrum of  $[\text{Fe}(\text{tpy-HImzPh}_3)_2]^{2+}$  is consistent with a symmetrical complex as shown by X-ray crystal structure in the solid state. Fig. 3(b) illustrates the effect of coordination of the  $\text{Fe}^{2+}$  center to the ligand on the chemical shift values of its different protons. It can be seen that the chemical shifts of H3, H7 and H8 protons are shifted downfield, while the phenyl protons and H4 of the terpyridine moiety are almost unaffected by coordination. Proton H6 of the tpy moiety is affected the most and shifts significantly upfield, because this proton lies above the shielding region of a pyridine ring of the other tpy ligand (Fig. 1).

### Absorption and emission spectral characteristics

The absorption and emission spectra of the receptor have been recorded in several solvents and the relevant spectral data in different solvents are given in Table 3. The absorption spectra of the receptor obtained in chloroform and dimethylformamide solutions are shown in Fig. 4. In all the solvents two intense bands are observed in the UV region; the lowest energy band ranges between  $285$  and  $356$  nm, while the higher energy band lies between  $269$  and  $286$  nm. The higher energy band seems to be due to a  $\pi$ – $\pi^*$  transition, while the lower energy band probably arises due to an intra-ligand charge transfer transition of the terpyridyl-imidazole ligand. It can be seen from Table 3 that the band maxima of the receptor shifts to longer wavelengths with an increase in polarity, as well as with the extent of the hydrogen bonding ability of the solvent (Fig. S2, ESI†). The effect of different solvents on the absorption and emission spectra of the Zn(II) complexes of the receptor have also been studied (Fig. S3, ESI†). The Zn(II) complex, of composition  $[\text{Zn}(\text{tpy-HImzPh}_3)_2]^{2+}$ , is prepared *in situ* by adding 0.5 equivalents of  $\text{Zn}(\text{ClO}_4)_2$  to the tpy-HImzPh<sub>3</sub> ligand. It is shown in Fig. 4 that the lowest-energy absorption band of

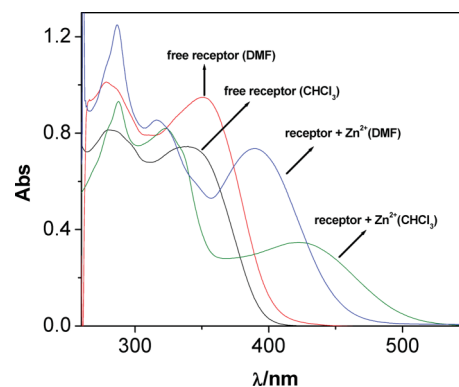


**Fig. 4** Absorption spectra of the receptor and its Zn(II) complex in chloroform and dimethylformamide solution.

**Table 3** Absorption and luminescence spectral data of the receptor and its Zn(II) complex in different solvents

Solvent	Free receptor				Zn(II) complex			
	Absorption $\lambda_{\max}$ , nm ( $\epsilon$ , M <sup>-1</sup> cm <sup>-1</sup> )	Emission			Absorption $\lambda_{\max}$ , nm ( $\epsilon$ , M <sup>-1</sup> cm <sup>-1</sup> )	Emission		
		$\lambda_{\max}$ , nm	$\tau$ , ns	$\Phi$		$\lambda_{\max}$ , nm	$\tau$ , ns	$\Phi$
CHCl <sub>3</sub>	335(br)(50 400) 286(br)(46 600)	448	1.61	0.084	427(15 800) 323(37 600) 287(42 600)	620	0.89 & 3.67	0.126
CH <sub>2</sub> Cl <sub>2</sub>	335(br)(31 100) 283(br)(30 500)	450	1.83	0.106	422(16 100) 325(39 700) 286(50 200)	613	1.12 & 3.37	0.08
DMF	353(br)(32 600) 278(br)(29 600)	487	2.56	0.096	389(36 800) 316(42 700) 286(62 500)	612	1.03 & 3.34	0.059
DMSO	356(br)(40 350) 278(br)(37 100)	492	2.63	0.1	394(26 700) 317(34 200) 288(46 600)	630	0.17 & 4.18	0.035
CH <sub>3</sub> OH	333(br)(34 000) 277(25 000)	515	0.72	0.012	389(23 700) 284(29 100)	610	0.55 & 2.55	0.03
(CH <sub>3</sub> ) <sub>2</sub> CO	350(br)(41 150)	472	2.60	0.11	402(32 500)	640	0.92 & 1.28	0.058
Hexane	285(br)(7700) 269(33 830)	415	1.25	0.088	—	—	—	—

the free ligand is red-shifted upon Zn<sup>2+</sup> complexation by Zn<sup>2+</sup> ion: the maximum in chloroform shifts from 335 to 427 nm. Coordination of the Zn<sup>2+</sup> ion serves to increase electron delocalization on the complex backbone, causing a red shift in the absorption.<sup>35,49</sup>

Upon excitation of either of the two absorption maxima, an intense emission band with a peak lying between 415 nm (hexane) and 515 nm (methanol) is observed. Fig. 5(a) and 5(b) show the absolute and normalized emission spectra of the receptor in different solvents. As compared with the absorption spectra, the emission spectral behavior shows significantly larger solvatochromism. The observed Stokes' shifts [( $v_{\text{abs}} - v_{\text{em}}$ )] can be ascribed to the distinct PCT effect. Fig. 5(c) shows the photograph of different emission colors (violet → blue → green → yellow) of the free ligand in different solvents upon excitation with UV light. It is interesting to note that as the emission colors were finely tuned from violet to blue to green to finally yellow; the receptor can act as a suitable solvent polarity indicator, *e.g.* a solvatochromic probe.<sup>49,50</sup> We have also studied the fluorescence decay behavior of the receptor in different solvents and the changes in decay profiles of the receptor as a function of solvent is represented in Fig. 6(a). In all cases, a single exponential fit to the decay profiles was found satisfactory from the  $\chi^2$  values and the residuals and the measured lifetime of the receptor lies in the range between 0.72 and 2.65 ns at room temperature. It is of interest to note that the lifetime of the receptor increases gradually with the increase in the polarity of the solvent, except in methanol.

The effect of complexation of Zn<sup>2+</sup> ion to the receptor is also reflected in the emission profiles in different solvents. Compared to the free receptor, its Zn(II) complex shows weak emission in the long wavelength region which probably originates from the ILCT state of [Zn(tpy-HImzPh<sub>3</sub>)<sub>2</sub>]<sup>2+</sup> (Fig. S3(b), ESI<sup>†</sup>).<sup>35,49,50</sup> The effect of different solvents on Zn<sup>2+</sup> complexes of the receptor has also been investigated by time-resolved fluorescence studies and the decay profiles are shown in Fig. 6(b). As compared with

single exponential decay of the free receptor, the Zn(II) complex exhibited complex kinetics that adequately fit with a sum of two exponentials. In general there is a gradual increase in the lifetime (2.25 to 4.18 ns) of the longer component as the polarity of the solvent increases, with the exception of methanol and acetone.

The electronic absorption spectrum of an acetonitrile solution of [Fe(tpy-HImzPh<sub>3</sub>)<sub>2</sub>]<sup>2+</sup> shows an intense band at 575 nm which is due to the Fe<sup>II</sup>(d $\pi$ )– $\pi^*$ (tpy-HImzPh<sub>3</sub>) MLCT transition. The absorption band is shifted to lower energy compared to the MLCT absorption of the parent [Fe(tpy)<sub>2</sub>]<sup>2+</sup> (551 nm) complex.<sup>51</sup> The electronic spectra of the complex also exhibits a series of higher energy absorptions arising from ligand centered  $\pi$ – $\pi^*$  and n– $\pi^*$  transitions. On excitation of any of its absorption bands, the iron complex does not exhibit luminescence at room temperature. It is well known in the literature that the photophysics of the polypyridine Fe(II) complex is complicated by the presence of ligand field (LF) excited states.<sup>34,51</sup> These states arise from population of the empty metal d $\sigma^*$  orbitals. Although optical transitions to yield the LF excited states are not dipole-allowed and are therefore of low probability, the LF states can become populated by crossing from the MLCT states. This occurs readily in polypyridine Fe(II) complexes where the LF state lies below the MLCT state.<sup>34,51</sup>

### Colorimetric signaling

The sensing ability of the receptor has been studied on a qualitative basis by visual examination of the anion- and cation-induced color changes in dimethylformamide-acetonitrile (1 : 9) solutions before and after the addition of anion and cation, respectively. Tetrabutylammonium salts of anions and hydrated perchlorate salts of the cations have been used as substrates for the receptor. The photograph in Fig. 7 shows the dramatic color changes of the receptor in the presence of F<sup>-</sup> and Fe<sup>2+</sup> ions in contrast to

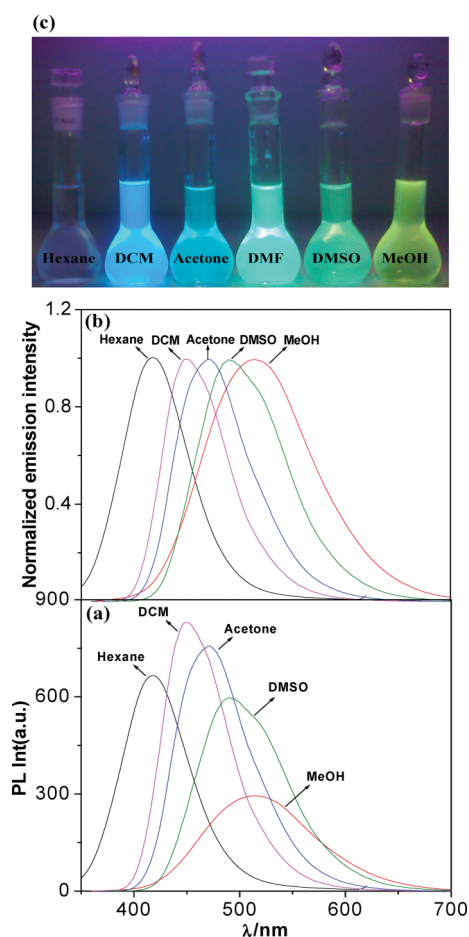


**Fig. 5** Fluorescence emission: absolute (a) normalized spectra (b) and different emission colors (c) seen upon excitation of the receptor with UV light in different solvents.

other anions and cations, respectively. The photograph shows that among the anions, only  $F^-$  and  $OH^-$  ions can cause evolution of a bright yellow color. On the other hand, addition of 0.5 equivalents of various metal ions to a solution of the receptor shows an appreciable change of color from colorless to deep violet only with  $Fe^{2+}$ . Other ions do not show such a dramatic color change, except for the appearance of a very light pink color in the case of  $Co^{2+}$  and a pale yellow color with the remaining metal ions. The visible color change of the receptor in the presence of  $F^-$  and  $Fe^{2+}$  can be useful for “naked-eye” detection of these ions in solution.

### Cation sensing

The sensing ability of the receptor for metal cations was studied through UV-vis spectra in dimethylformamide-acetonitrile (1 : 9) solutions. Fig. 8 shows the changes in the spectral profiles of the receptor following the addition of 0.5 equivalents of different metal ions. It is of interest to note that following addition of  $Fe^{2+}$  a strong MLCT band originates at 575 nm with the evolution of a bright violet color, in contrast to other metal ions. Whereas the cobalt complex also shows much weaker absorption in the visible region ( $\lambda > 400$  nm) due to metal-to-ligand charge-transfer absorption, the complexes of other metals either absorb weakly in this area or do not show any absorptions at wavelengths higher than 390 nm. Interestingly, these events can be distinguished visually as shown

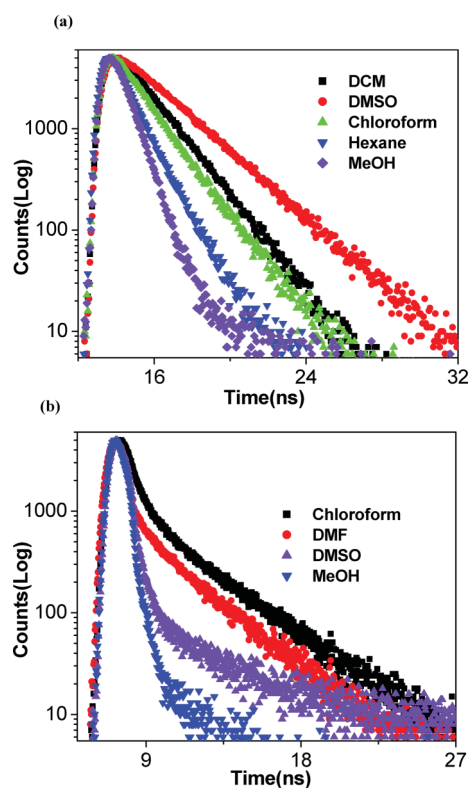


**Fig. 6** Time-resolved fluorescence decay profiles of the free receptor (a) and its Zn(II) complex (b) in different solvents.



**Fig. 7** Color changes that occur when the dimethylformamide-acetonitrile (1 : 9) solutions of the receptor are treated with (a) various anions as their tetrabutylammonium (TBA) salts and (b) various metal cations as their perchlorate salts.

in the picture (Fig. 7). A predominant spectral red-shift from 340 nm to 575 nm in the case of  $Fe^{2+}$  over the other metal ions suggests that the receptor can act as an effective chemosensor towards the detection of  $Fe^{2+}$  in solution.

It is of interest to assess the colorimetric sensing ability of the receptor towards different cationic guests. In order to do so, UV-vis titration of tpy-HImzPh<sub>3</sub> with different transition metal cations was carried out in dimethylformamide-acetonitrile (1 : 9). The absorption spectral changes were recorded between 250 and 700 nm for solutions in which the concentration of

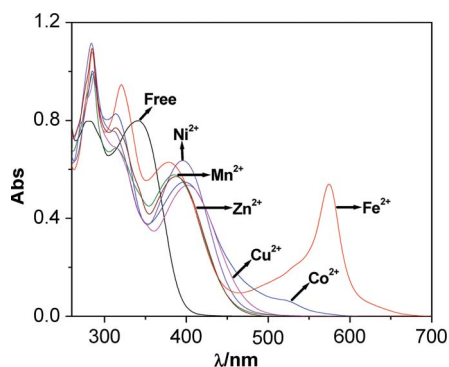


**Fig. 8** Changes in UV-vis spectra of the receptor in dimethylformamide-acetonitrile (1 : 9) upon the addition of different metal ions.

ligand was kept fixed ( $2 \times 10^{-5}$  M), while the concentrations of metal perchlorates were increased progressively until the limiting spectrum was reached, when no further changes in absorbance occurred. Fig. 9(a) and 9(c) show the spectral changes that take place upon the addition of increasing amounts of  $\text{Fe}(\text{ClO}_4)_2$  and  $\text{Zn}(\text{ClO}_4)_2$  to the receptor, respectively. As may be noted, the new band centered at 575 nm increases linearly with the incremental addition of  $\text{Fe}^{2+}$  ion until the  $[\text{Fe}^{2+}]/[\text{tpy-HImzPh}_3]$  reaches 0.5. Even higher concentrations of  $\text{Fe}^{2+}$  do not lead to any further change. The titration profile based on absorbance at 575 nm and the clear isosbestic points at 364, 331 and 273 nm imply the single conversion of free  $\text{tpy-HImzPh}_3$  to  $[\text{Fe}(\text{tpy-HImzPh}_3)_2]^{2+}$ . In contrast to  $\text{Fe}^{2+}$ , no color changes occurred for  $\text{Fe}^{3+}$ , indicating the lack of associative behavior of the receptor with trivalent iron. On the other hand, with the progressive addition of  $\text{Zn}(\text{ClO}_4)_2$ ,

diminution of the intensity of the major peak at 341 nm with a simultaneous increase in absorbance at 390 and 285 nm occurs. In this case, successive absorption curves pass through well-defined isosbestic points at 368 and 324 nm. The red-shift of the absorption band in the  $\text{Zn}(\text{II})$  complex could be attributed to the  $\text{Zn}(\text{II})$ -induced intraligand charge transfer (ILCT) process from the triphenyl imidazole group to the tpy moiety, because coordinated tpy is a better electron acceptor than the free tpy moiety of the ligand.

For all metal ions, distinct changes in tpy absorption were observed upon complexation and clear isosbestic points were found (Fig. 9 and Fig. S4–S9, ESI†), indicating that only a single equilibrium between two species, namely free and complexed  $\text{tpy-HImzPh}_3$ , occurs during the titration. Whereas the iron complex shows intense absorption in the visible region due to metal-to-ligand charge-transfer absorption, the complexes of other metal ions only absorb very weakly in this area. Absorption titration profiles of the free receptor with various metal ions (Fig. 9 and Fig. S4–S9, ESI† insets) show a linear increase and a sharp endpoint at a metal/ligand ratio of 0.5 : 1, indicating the formation of a  $[\text{M}(\text{tpy-HImzPh}_3)_2]^{2+}$  (1 : 2) complex. Due to the lack of curvature in the titration curve, no binding constants could be determined.<sup>33c,52</sup>

The sensitivity and selectivity of the bifunctional receptor for different metal ions have also been studied. Spectrophotometric measurements in the presence of competing cations have been performed by treating a solution of  $\text{tpy-HImzPh}_3$  ( $c = 2.0 \times 10^{-5}$  M) with 0.5 equivalents of  $\text{Fe}^{2+}$  in the presence of each of the other metal ions *viz.*  $\text{Mn}^{2+}$ ,  $\text{Co}^{2+}$ ,  $\text{Ni}^{2+}$ ,  $\text{Cu}^{2+}$ ,  $\text{Zn}^{2+}$ ,  $\text{Pb}^{2+}$ , and  $\text{Cd}^{2+}$ . In the competition experiments, we are still able to observe

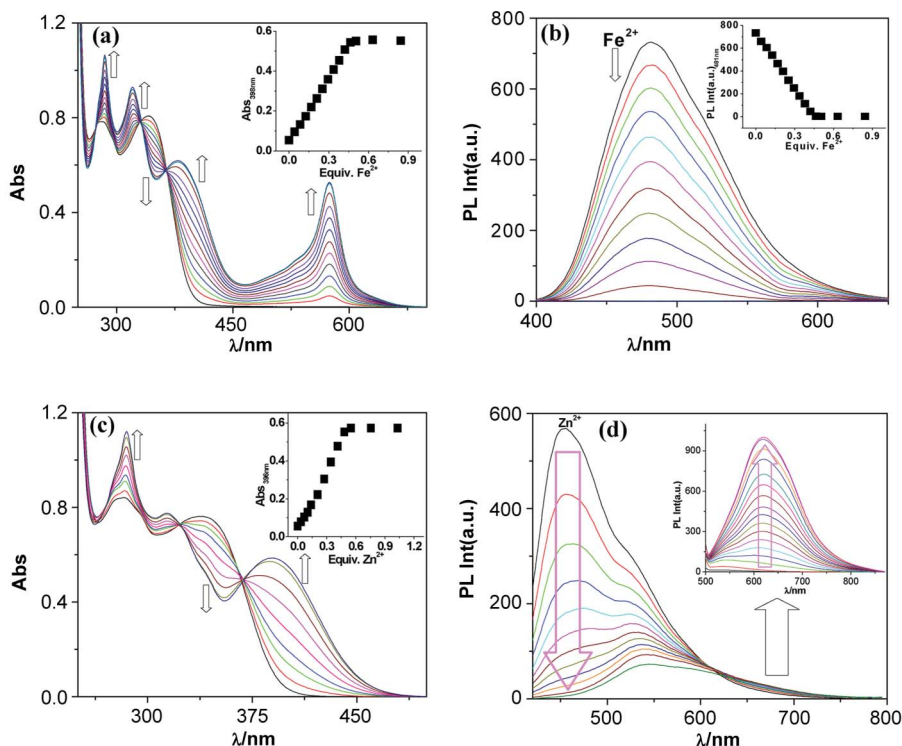


**Fig. 9** Changes in UV-vis (a, c) and photoluminescence (b, d) spectra of  $\text{tpy-HImzPh}_3$  in dimethylformamide-acetonitrile (1 : 9) upon addition of  $\text{Fe}(\text{ClO}_4)_2$  and  $\text{Zn}(\text{ClO}_4)_2$ . The inset shows the change of absorption and emission intensity as a function of the equivalents of  $\text{Fe}^{2+}$  and  $\text{Zn}^{2+}$  ions added.

the band at 575 nm due to  $\text{Fe}^{2+}$  MLCT, though the intensity is a little lower compared with  $[\text{Fe}(\text{tpy-HImzPh}_3)_2]^{2+}$  alone. The results clearly indicate that the terpyridyl-imidazole receptor has a high selectivity for  $\text{Fe}^{2+}$  over other metal ions. The selectivity of the receptor for  $\text{Fe}^{2+}$  over other metal ions can also be judged by comparing the epsilon ( $\epsilon$ ) values of the Fe-complex with those of the other metal complexes at a given wavelength. Table S3, ESI† shows the  $\epsilon$  values of complexes of different metal ions under investigation at three different wavelengths, assuming that only two species ( $\text{tpy-HImzPh}_3$ ) and  $[\text{M}(\text{tpy-HImzPh}_3)_2]^{2+}$  exist in solution, and there is no reason to believe that significant amounts of intermediate complexes will exist other than the homoleptic metal complexes at low metal concentrations. Much higher  $\epsilon$  values of the Fe-complex over the others at a given wavelength suggests that the receptor can act as an effective and selective sensor towards the detection of  $\text{Fe}^{2+}$  over other metals in solution.

Fluorescence titration of the receptor with different metal cations was also investigated. Fig. 9(b) and 9(d) show the quenching of emission intensity of the receptor on incremental addition of  $\text{Fe}(\text{ClO}_4)_2$  and  $\text{Zn}(\text{ClO}_4)_2$ , respectively. The insets of Fig. 9 indicate that complete quenching occurs at 0.5 equiv. of both the metal ions. It is interesting to note that coordination of the metal ions triggers the emission quenching of the receptor in all cases except with  $\text{Zn}^{2+}$ . In the case of  $\text{Zn}^{2+}$ , gradual quenching of the fluorescence intensity at 448 nm accompanied by a distinct linear emission enhancement at 620 nm occurs with the incremental addition of  $\text{Zn}^{2+}$  ion (Fig. 9(d)). The emission at 620 nm probably arises from the ILCT state of  $[\text{Zn}(\text{tpy-HImzPh}_3)_2]^{2+}$  complex.<sup>35</sup>

The electrochemical  $\text{Fe}^{2+}$  ion recognition and sensing of the receptor in dimethylformamide-acetonitrile have been examined using cyclic and square wave voltammetry. As shown in Fig. 10(a), with progressive addition of  $\text{Fe}^{2+}$  to the receptor, a new redox couple is observed at 1.10 V (Pt working electrode) due to the  $\text{Fe}^{\text{II}}/\text{Fe}^{\text{III}}$  oxidation process, and gradually increases in current height until the receptor: $\text{Fe}^{2+}$  ratio reaches 2:1. The change in current height for the redox couple with the variation of concentration of added  $\text{Fe}^{2+}$  ion is shown in Fig. 10(b). On addition of excess  $\text{Fe}^{2+}$  ions to the solution of the receptor, a new oxidation peak is generated at 1.16 V (Fig. S10, ESI†) in the vicinity of the original peak at 1.10 V. The evolution of a new oxidation couple following further addition of  $\text{Fe}^{2+}$  may be associated with gradual formation of mono-terpyridyl Fe(II) complexes.

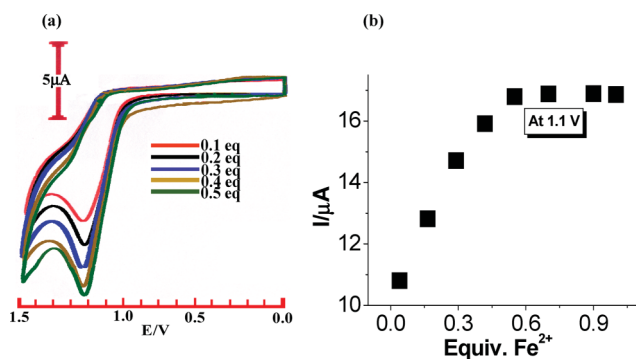


**Fig. 10** CVs (a) obtained upon incremental addition of  $\text{Fe}(\text{ClO}_4)_2$  to a dimethylformamide-acetonitrile (2 : 3) solution of the receptor ( $1.0 \times 10^{-3}$  M). The change in the current intensities as a function of equivalents of  $\text{Fe}^{2+}$  ion added is shown in (b).

The electrochemical response of the sensor in the presence of  $\text{Fe}^{2+}$  ion in the negative potential window 0 to  $-1.7$  V has also been observed with a glassy carbon working electrode. The cyclic voltammogram of the free receptor shows an irreversible reduction at  $-0.82$  V with very low current intensity. Incremental addition of  $\text{Fe}^{2+}$  ion to the solution of the receptor resulted in two successive one-electron quasi-reversible reductions at  $-1.10$  and  $-1.20$  V (Fig. 11).

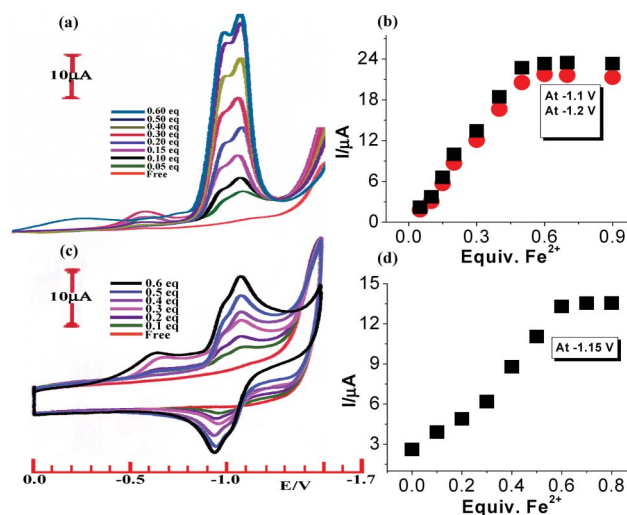


**Fig. 11** SWVs (a) and CVs (b) obtained upon incremental addition of  $\text{Fe}(\text{ClO}_4)_2$  to a dimethylformamide-acetonitrile (2 : 3) solution of the receptor in the negative potential window. The changes in the current intensities as a function of equivalents of  $\text{Fe}^{2+}$  ion added are shown in (b) and (d), respectively.

It should be noted that the current intensity associated with the new reduction peaks at  $-1.10$  and  $-1.20$  V due to  $\text{Fe}^{2+}$ -bound receptor gradually increases and reaches a limit when approximately 0.5 equiv. of  $\text{Fe}^{2+}$  ion had been added to the receptor. The observed redox behavior is in consonance with the behavior of the isolated  $[\text{Fe}(\text{tpy-HImzPh}_3)_2]^{2+}$  compound (Fig. S11, ESI†).

### Anion sensing

Sensing of the anions by the receptor has been monitored by observing the spectral changes that occur in dimethylformamide-acetonitrile (1 : 9) solutions. As shown in Fig. 12(a), the peaks at 341 and 281 nm remain practically unchanged upon addition of 10 equiv. of  $\text{Cl}^-$ ,  $\text{Br}^-$ ,  $\text{I}^-$ ,  $\text{AcO}^-$ ,  $\text{H}_2\text{PO}_4^-$ , and  $\text{ClO}_4^-$  ions to  $2.0 \times 10^{-5}$  M solutions of the receptor. On the other hand, following the addition of excess  $\text{F}^-$ , the band at 341 nm is red-shifted to 420 nm, indicating that strong interactions occur between the receptor and  $\text{F}^-$  ion. Again, Fig. 12(b) shows that the emission intensity of the band at 482 nm undergoes a nominal change with the addition of all the anions except for  $\text{F}^-$ . With a ten-fold addition of  $\text{F}^-$  ion, the emission intensity is completely quenched. Thus, the absorbance and luminescence behavior of the receptor towards the anions shows a close similarity. These observations are in consonance with the visual changes already noted in Fig. 7. The red-shift of the spectral band can be attributed to anion-induced deprotonation of the imidazole NH proton of the receptor, which increases the

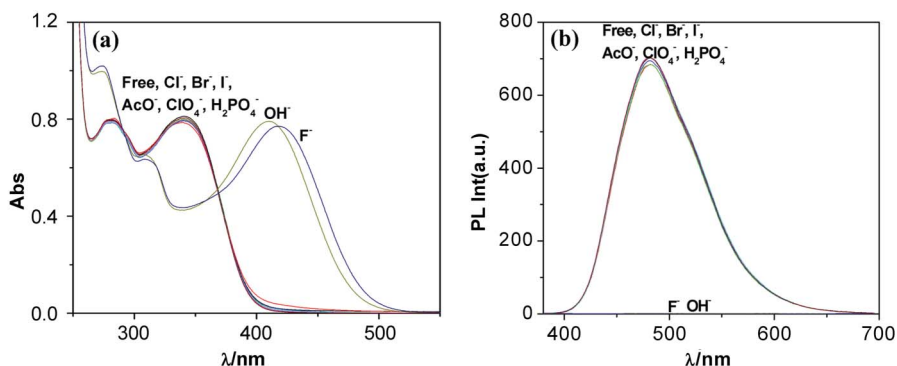


**Fig. 12** Changes in UV-vis (a) and luminescence (b) spectra of tpy-HImzPh<sub>3</sub> in dimethylformamide-acetonitrile (1 : 9) solution upon the addition of different anions as TBA salts.

electron density at the imidazole fragment leading to a lowering of the band energy.<sup>53</sup>

In order to obtain quantitative insight into the sensor-anion interaction, spectrophotometric titration experiments were carried out with tpy-HImzPh<sub>3</sub> in dimethylformamide-acetonitrile (1 : 9) and various anions. Fig. 13(a) presents the changes in the UV-vis spectrum of tpy-HImzPh<sub>3</sub> as a function of F<sup>-</sup> ion. As can be seen, the intensity of the peak at 341 nm decreases gradually with a simultaneous increase of the band at 420 nm, with the appearance of two isosbestic points at 370 and 284 nm after the addition of excess F<sup>-</sup>. Furthermore, the color of the solution was seen to change from colorless to yellow. Standard curve-fitting procedures were then used to derive a binding/equilibrium constant ( $1.9 \times 10^4 \text{ M}^{-1}$ ). Spectrophotometric titration of the ligand was also carried out with TBAOH. The spectral pattern obtained with OH<sup>-</sup> (Fig. S12(a), ESI<sup>†</sup>) has a close resemblance to the spectra of the receptor with F<sup>-</sup>. The result probably indicates that the imidazole NH is deprotonated with a large excess of F<sup>-</sup> ions.

Photoluminescence titrations of the receptor with various anions have been carried out in the same way as already described for spectrophotometric measurements. In Fig. 13(b), the effect of incremental addition of F<sup>-</sup> ions to the receptor is shown and the inset shows that almost complete quenching of luminescence intensity occurs at *ca.* 10 equivalents. The change in the emission spectrum of tpy-HImzPh<sub>3</sub> as a function of OH<sup>-</sup> is also shown in Fig. S10(b), ESI<sup>†</sup>.

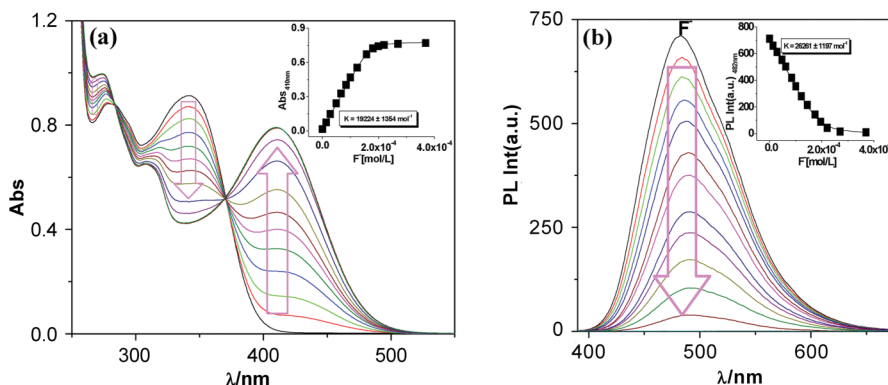


**Fig. 13** Changes in UV-vis (a) and luminescence (b) spectra of tpy-HImzPh<sub>3</sub> in dimethylformamide-acetonitrile (1 : 9) upon the addition of F<sup>-</sup> ion. The insets show the fit of the experimental absorbance and luminescence data to a 1 : 1 binding profile.

It is to be noted that the very high affinity of fluoride toward imidazole N–H may be due to the very high stability of the HF<sub>2</sub><sup>-</sup> complex, whose formation allows N–H deprotonation.<sup>53</sup> The appearance of bright yellow colors following deprotonation of the N–H proton does not prevent from the colorimetric determination of the F<sup>-</sup> ion in solution by the terpyridyl-imidazole derivative, which is indeed very efficient and suffers from the interference of only one analyte, OH<sup>-</sup>.<sup>53</sup>

The electrochemical F<sup>-</sup> ion sensing of the receptor has also been examined by cyclic and square wave voltammetry. It is interesting to note that with progressive addition of F<sup>-</sup> to the receptor, contrary to that of the free receptor, a fully reversible reduction wave appeared at  $E_{1/2} = -0.77 \text{ V}$  and the current height of this couple grows gradually until 10 equiv. of F<sup>-</sup> ion is added (Fig. 14). A similar electrochemical response is also observed upon addition of OH<sup>-</sup> ion. In contrast to F<sup>-</sup> and OH<sup>-</sup>, no noticeable changes occur in electrochemical responses for the receptor in the presence of a large excess of other anions such as Cl<sup>-</sup> and AcO<sup>-</sup>. The results indicate that the receptor could prove useful in the fabrication of an electrochemical sensor for both Fe<sup>2+</sup> and F<sup>-</sup> ions.

### Sensing in the presence of competing ions

Since tpy-HImzPh<sub>3</sub> contains two binding sites for the metal ions and anion, we investigated the effect of competing F<sup>-</sup> ion on the binding ability of tpy-HImzPh<sub>3</sub> for metal ions and *vice*

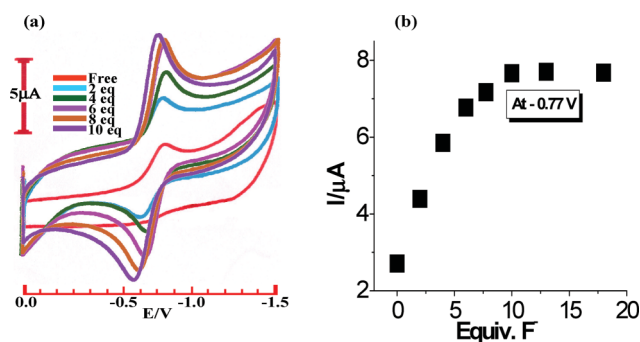


**Fig. 14** CVs (a) obtained upon incremental addition of  $F^-$  ion to a dimethylformamide-acetonitrile (2:3) solution of the receptor in the negative potential window. The change in the current intensities as a function of equivalents of  $F^-$  ion added is shown in (b).

*versa*. Two different strategies were adopted for carrying out these experiments. First, we have titrated  $\text{tpy-HImzPh}_3$  with  $F^-$  in the presence of 0.5 equivalents of metal ions. Second, we have titrated  $\text{tpy-HImzPh}_3$  with  $M^{2+}$  in the presence of 10 equivalents of  $F^-$  ion. Initially,  $Fe^{2+}$  and  $F^-$  were used for the dual sensing studies. Spectrophotometric measurements (Fig. 15) show that the addition of  $F^-$  to the  $\text{tpy-HImzPh}_3 \cdot Fe^{2+}$  complex did not lead to any significant red-shifts of the MLCT band (due to anion-induced

deprotonation of the imidazole NH protons), rather resulting in a gradual reduction of the intensity of the band at 575 nm with concomitant change of color from violet to colorless with up to 3 equivalents of  $F^-$  ion. Further addition of  $F^-$  beyond 3 equivalents leads to enhancement of the intensity of the band at 420 nm with the development of a bright yellow color, similar to that observed upon the addition of  $F^-$  ion to the free receptor. Photoluminescence titrations of the  $\text{tpy-HImzPh}_3 \cdot Fe^{2+}$  complex with incremental addition of  $F^-$  is shown in Fig. 15(e). As already mentioned, the  $\text{tpy-HImzPh}_3 \cdot Fe^{2+}$  complex is non-luminescent at room temperature. Upon the addition of 3 equivalents of  $F^-$ , significant enhancement of emission at 482 nm (corresponding to that of the free receptor) (Fig. 15(d)) occurs. Upon the addition of an excess of  $F^-$  (up to 13 equivalents), the emission of said band is again completely quenched (Fig. 15(f)). These data clearly indicate that addition of the first few equivalent of  $F^-$  leads to sequestering of the  $Fe^{2+}$  ion from the receptor to form a more stable ion-pair or complex cation in solution, and anion binding by the receptor is effectively inhibited by this process.<sup>24b,54,55</sup> But in the presence of excess  $F^-$  ion, when sequestering of the metal ion is complete, deprotonation of the imidazole NH proton of  $\text{tpy-HImzPh}_3$  occurs. We repeated similar experiments with  $Zn^{2+}$  and  $F^-$  (shown in Fig. S14, ESI<sup>†</sup>), as  $Zn^{2+}$  salts are colorless and it is possible to observe distinct changes due to metal coordination or

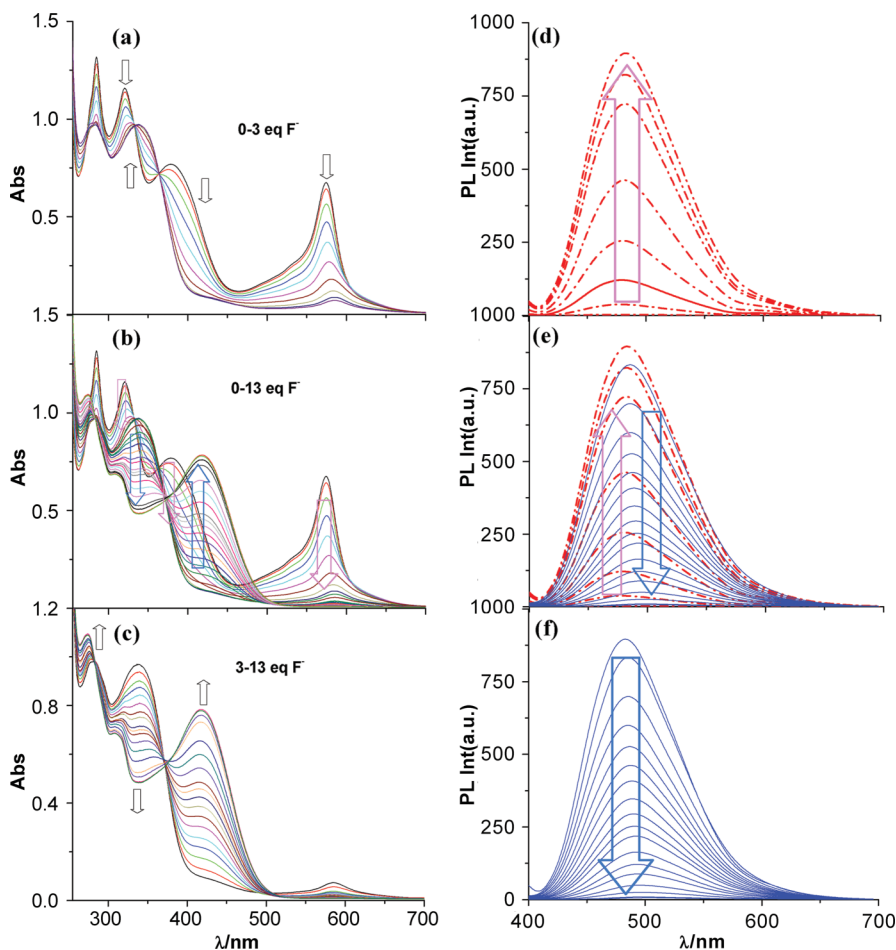


**Fig. 15** Changes in UV-vis (a–c) and photoluminescence (d–f) spectra of  $\text{tpy-HImzPh}_3 \cdot Fe^{2+}$  in dimethylformamide-acetonitrile (1:9) upon incremental addition of  $F^-$  ion.

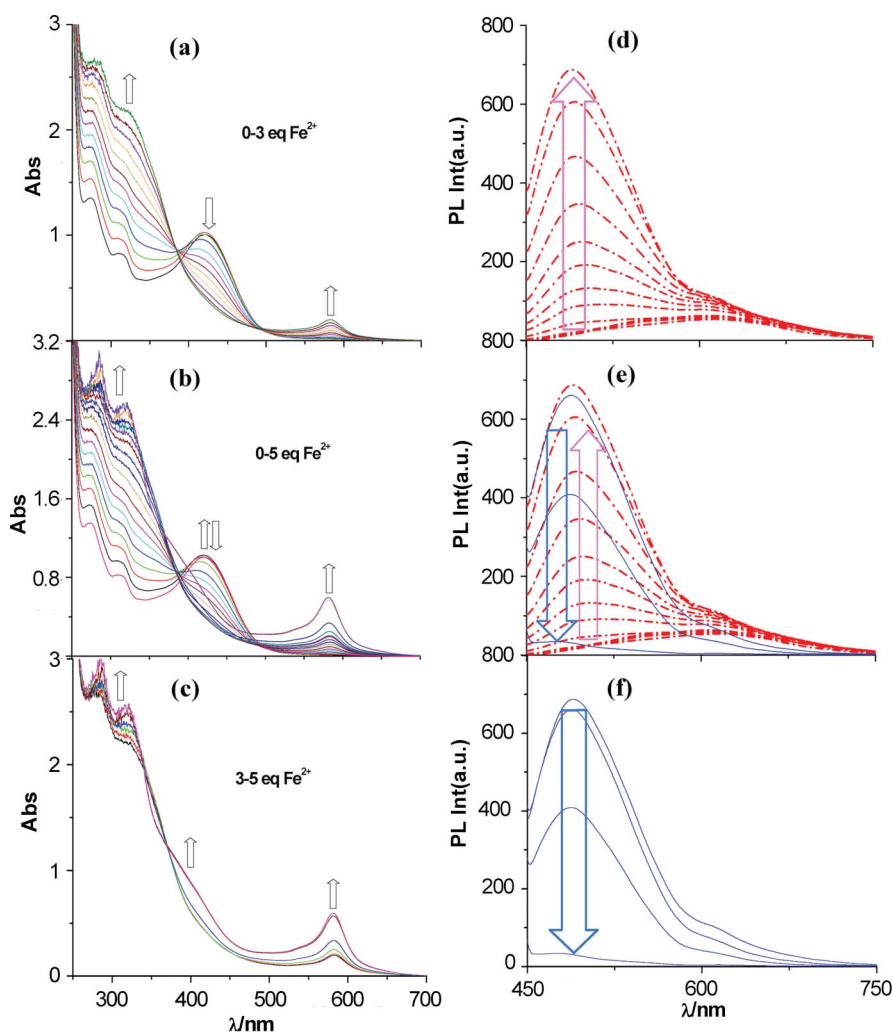


**Fig. 16** Changes in UV-vis (a–c) and photoluminescence (d–f) spectra of tpy-HImzPh<sub>3</sub>·F<sup>-</sup> in dimethylformamide-acetonitrile (1 : 9) upon incremental addition of Fe<sup>2+</sup> ion.

decoordination without any interference from the color of the salts. As can be seen, initial titration of tpy-HImzPh<sub>3</sub> and 0.5 equivalents of Zn<sup>2+</sup> with F<sup>-</sup> results in a drastic reduction of the intensity of the absorption band at 394 nm, suggesting sequestering of the metal ion to form an ion pair with F<sup>-</sup> ion in solution.<sup>24b,54,55</sup> However, when sequestering of the metal ion is complete, further addition of F<sup>-</sup> ion leads to enhancement of the intensity of the band at 420 nm. The emission spectral behavior of the tpy-HImzPh<sub>3</sub>·Zn<sup>2+</sup> complex as function of F<sup>-</sup> is shown in Fig. S14(b), ESI.†

In the second category of experiment (shown in Fig. 16), which is carried out in the presence of 10 equivalents of F<sup>-</sup>, addition of either Fe<sup>2+</sup> or Zn<sup>2+</sup> ion leads to a gradual reduction of the intensity of the absorption band at 420 nm, due to the sequestering of F<sup>-</sup> ion. The presence of excess of F<sup>-</sup> in the solution engages the metal ions in ion pair and/or complex formation in solution rather than engaging them in complexation with the receptor. As shown in Fig. 16, the enhancement of the intensity of the band at 583 nm for the Fe<sup>2+</sup> complex occurs only after addition of more than 3 equivalents of Fe<sup>2+</sup> ion. It is to be noted that the absorption spectral behavior in the UV region differs from that of the receptor (either in the presence of excess F<sup>-</sup> or Fe<sup>2+</sup>). We performed a blank

experiment by adding incremental amounts of Fe<sup>2+</sup> to a solution (DMF-MeCN) containing excess F<sup>-</sup> ion and we observed that the species generated (ion-pair/complex species) absorb moderately in the UV region. The sensing studies in the presence of competing ions indicate that although tpy-HImzPh<sub>3</sub> contains distinct binding sites for both anion and cation, simultaneous binding of both the species is not possible in this case, unless the total concentration of the two species is much lower than that a particular binding site can accommodate.

## Conclusions

In conclusion, we have developed a new sensor 4'-[4-(4,5-diphenyl-1*H*-imidazol-2-yl)-phenyl]-[2,2':6',2'']terpyridine, where the terpyridine moiety has been utilized as the cation binding site and the imidazole motif as the anion binding site. The receptor can act as colorimetric sensor for Fe<sup>2+</sup> and F<sup>-</sup> ions in solution. The binding properties have been confirmed by absorption, emission and <sup>1</sup>H NMR spectroscopic techniques and also by electrochemical studies. The binding site for the Fe<sup>2+</sup> ion in the system has been unambiguously established by single-crystal X-ray diffraction

study of the Fe(II) complex of the receptor. Anion sensing studies indicate that in the presence of excess F<sup>-</sup>, deprotonation of the imidazole N–H proton of the receptor occurs with the development of a bright yellow color. It is gratifying to note that the terpyridylimidazole ligand behaves as a triple-channel sensor for both Fe<sup>2+</sup> and F<sup>-</sup> ions in solution. It is also interesting to note that, as the emission color of the receptor was finely tuned from violet to blue to green to finally yellow, the receptor can act as a suitable solvatochromic probe.

## Acknowledgements

Financial assistance received from the Department of Science and Technology, New Delhi [Grant No. SR/S1/IC-33/2010] and the Council of Scientific and Industrial Research, New Delhi, India [Grant No. 01(2084)/06/EMR-II], is gratefully acknowledged. Thanks are due to the DST for providing a single crystal X-ray diffractometer in FIST and a Time-Resolved Nanosecond Spectrofluorimeter in the PURSE programme at the Department of Chemistry of Jadavpur University. C.B., S.D. and D.M thank CSIR for their fellowships.

## References

- J. L. Sessler, P. A. Gale and W. S. Cho, *Anion Receptor Chemistry*, Royal Society of Chemistry, Cambridge, U.K., 2006.
- (a) *Supramolecular Chemistry of Anions*, (Eds. A. Bianchi, K. Bowman-James and E. Garcia-España), Wiley-VCH, New York, 1997; (b) K. Bowman-James, *Acc. Chem. Res.*, 2005, **38**, 671.
- T. Schrader and A. D. Hamilton, *Functional Synthetic Receptors*, Wiley-VCH, Weinheim, Germany, 2005.
- (a) J.-M. Lehn, *Supramolecular Chemistry, Concepts and Perspective*, VCH, Weinheim, Germany, 1995; (b) V. Balzani, A. Juris and M. Venturi, *Chem. Rev.*, 1996, **96**, 759; (c) A. P. de Silva, H. Q. N. Gunaratne, T. Gunnlaugsson, A. J. M. Huxley, C. P. McCoy, J. T. Rademacher and T. E. Rice, *Chem. Rev.*, 1997, **97**, 1515.
- (a) C. Caltagirone and P. A. Gale, *Chem. Soc. Rev.*, 2009, **38**, 520; (b) P. A. Gale, S. E. Garcia-Garrido and J. Garric, *Chem. Soc. Rev.*, 2008, **37**, 151; (c) P. D. Beer, *Chem. Commun.*, 1996, 689; (d) P. D. Beer and P. A. Gale, *Angew. Chem., Int. Ed.*, 2001, **40**, 486; (e) P. A. Gale, *Coord. Chem. Rev.*, 2006, **250**, 2917; (f) P. A. Gale, *Coord. Chem. Rev.*, 2003, **240**, 226; (g) J. L. Sessler and J. M. Davis, *Acc. Chem. Res.*, 2001, **34**, 989.
- R. Martínez-Mañez and F. Sancenón, *Chem. Rev.*, 2003, **103**, 4419.
- (a) P. D. Beer, *Coord. Chem. Rev.*, 2000, **205**, 131; (b) S.-S. Sun and A. J. Lees, *Coord. Chem. Rev.*, 2002, **230**, 171; (c) C. Suksai and T. Tuntulani, *Top. Curr. Chem.*, 2005, **255**, 163; (d) C. Suksai and T. Tuntulani, *Chem. Soc. Rev.*, 2003, **32**, 192.
- V. Amendola, E. D. Gómez, L. Fabbri and M. Licchelli, *Acc. Chem. Res.*, 2006, **39**, 343.
- (a) J. Pérez and L. Riera, *Chem. Commun.*, 2008, 533; (b) J. Pérez and L. Riera, *Chem. Soc. Rev.*, 2008, **37**, 2658.
- (a) J. W. Steed, *Chem. Soc. Rev.*, 2009, **38**, 506.
- (a) C. M. G. dos Santos, A. J. Harte, S. T. Quinn and T. Gunnlaugsson, *Coord. Chem. Rev.*, 2008, **252**, 2512; (b) T. Gunnlaugsson, M. Glynn, G. M. (nee Hussey), Tocci, P. E. Kruger and F. M. Pfeffer, *Coord. Chem. Rev.*, 2006, **250**, 3094; (c) J. P. Leonard, C. B. Nolan, F. Stomeo and T. Gunnlaugsson, *Top. Curr. Chem.*, 2007, **281**, 1.
- (a) I. Bertini, H. B. Gray, S. J. Lippard and J. S. Valentine, *Bioinorganic Chemistry*, University Science Book, Mill Valley, CA, 1994; (b) E. M. Nolan and S. J. Lippard, *Chem. Rev.*, 2008, **108**, 3443.
- F. A. Cotton and G. Wilkinson, *Advanced Inorganic Chemistry*, 5th Ed. Wiley-Interscience Publication, John-Wiley & Sons, 1988.
- N. N. Greenwood and A. Earnshaw, *Chemistry of the Elements*: Maxwell Macmillan International Edn, 1989.
- (a) D. W. Domaille, E. L. Que and C. J. Chang, *Nat. Chem. Biol.*, 2008, **4**, 168; (b) A. P. de Silva, D. B. Fox and A. J. M. Huxley, *Coord. Chem. Rev.*, 2000, **205**, 41; (c) A. Czarnik, *Fluorescent Chemosensors for Ion and Molecule Recognition*, W. Ed., American Chemical Society, Washington, D.C., 1992; (d) P. Jiang and Z. Guo, *Coord. Chem. Rev.*, 2004, **248**, 205; (e) H. M. Kim and B. R. Cho, *Acc. Chem. Res.*, 2009, **42**, 863; (f) Z. Xu, J. Yoon and D. R. Spring, *Chem. Soc. Rev.*, 2010, **39**, 1996.
- (a) X. He and V. W. W. Yam, *Org. Lett.*, 2011, **13**, 2172; (b) X. He and V. W. W. Yam, *Inorg. Chem.*, 2010, **49**, 2273; (c) S.-T. Lam, N. Zhu and V. W. W. Yam, *Inorg. Chem.*, 2009, **48**, 9664; (d) M. J. Li, B. W. K. Chu and V. W. W. Yam, *Chem.–Eur. J.*, 2006, **12**, 3528; (e) M. J. Li, C. C. Ko, G. P. Duan, N. Zhu and V. W. W. Yam, *Organometallics*, 2007, **26**, 6091.
- (a) M. T. Reetz, C. M. Niemeyer and K. Harms, *Angew. Chem., Int. Ed. Engl.*, 1991, **30**, 1474; (b) D. J. White, N. Laing, H. Miller, S. Parsons, S. Coles and P. A. Tasker, *Chem. Commun.*, 1999, 2077; (c) X. Shi, J. C. Fettinger and J. T. Davis, *Angew. Chem., Int. Ed.*, 2001, **40**, 2827; (d) G. Domenico, G. Giuseppe, N. Anna, P. Andrea, P. Sebastiano, F. P. Melchiorre, P. Marta and P. Ilenia, *Angew. Chem., Int. Ed.*, 2005, **44**, 4892; (e) M. Cametti, M. Nissinen, A. Dalla Cort, L. Mandolini and K. Rissanen, *J. Am. Chem. Soc.*, 2007, **129**, 3641.
- (a) J. M. Mahoney, K. A. Stucker, H. Jiang, I. Carmichael, N. R. Brinkmann, A. M. Beatty, B. C. Noll and B. D. Smith, *J. Am. Chem. Soc.*, 2005, **127**, 2922; (b) M. J. Deetz, M. Shang and B. D. Smith, *J. Am. Chem. Soc.*, 2000, **122**, 6201; (c) J. M. Mahoney, A. M. Beatty and B. D. Smith, *Inorg. Chem.*, 2004, **43**, 7617.
- (a) M. P. Wintergerst, T. G. Levitskaia, B. A. Moyer, J. L. Sessler and L. H. Delmau, *J. Am. Chem. Soc.*, 2008, **130**, 4129; (b) J. L. Sessler, S. K. Kim, D. E. Gross, C.-H. Lee, J. S. Kim and V. M. Lynch, *J. Am. Chem. Soc.*, 2008, **130**, 13162.
- (a) K. Niikura and E. V. Anslyn, *J. Org. Chem.*, 2003, **68**, 10156; (b) S. L. Tobey and E. V. Anslyn, *J. Am. Chem. Soc.*, 2003, **125**, 10963.
- (a) M. D. Lankshear, I. M. Dudley, K.-M. Chan and P. D. Beer, *New J. Chem.*, 2007, **31**, 684; (b) M. D. Lankshear, I. M. Dudley, K.-M. Chan, A. R. Cowley, S. M. Santos, V. Felix and P. D. Beer, *Chem.–Eur. J.*, 2008, **14**, 2248.
- Z. Yang, C. Yan, Y. Chen, C. Zhu, C. Zhang, W. Y. Dong, Z. Guo, Y. Lu and W. He, *Dalton Trans.*, 2011, **40**, 2173.
- (a) Z. Q. Liang, C. X. Wang, J. X. Yang, H. W. Gao, Y. P. Tian, X. T. Taoc and M. H. Jiang, *New J. Chem.*, 2007, **31**, 906; (b) Y. Gao, J. Wu, Q. Zhao, L. Zheng, H. Zhou, S. Zhang, J. Yang and Y. Tian, *New J. Chem.*, 2009, **33**, 607; (c) Z. J. Hu, J. X. Yang, Y. P. Tian, X. T. Tao, L. Tian, H. P. Zhou, G. B. Xu, W. T. Yu, Y. X. Yan, Y. H. Sun, C. K. Wang, X. Q. Yu and M. H. Jiang, *Bull. Chem. Soc. Jpn.*, 2007, **80**, 986.
- (a) T. Ábalos, D. Jiménez, M. Moragues, S. Royo, R. Martínez-Mañez, F. Sancenón, J. Soto, A. M. Costero, M. Parra and S. Gil, *Dalton Trans.*, 2010, **39**, 3449; (b) T. Ghosh, B. G. Maiya and A. Samanta, *Dalton Trans.*, 2006, 795.
- (a) J. S. Kim and D. T. Quang, *Chem. Rev.*, 2007, **107**, 3780; (b) J. Y. Lee, S. K. Kim, J. H. Jung and J. S. Kim, *J. Org. Chem.*, 2005, **70**, 1463; (c) J. L. Sessler, S. K. Kim, D. E. Gross, C.-H. Lee, J. S. Kim and V. M. Lynch, *J. Am. Chem. Soc.*, 2008, **130**, 13162; (d) M. H. Lee, D. T. Quang, H. S. Jung, J. Yoon, C.-H. Lee and J. S. Kim, *J. Org. Chem.*, 2007, **72**, 4242.
- (a) S. C. Burdette and S. J. Lippard, *Coord. Chem. Rev.*, 2000, **216–217**, 333; (b) D. Buccella, J. A. Horowitz and S. J. Lippard, *J. Am. Chem. Soc.*, 2011, **133**, 4101; (c) L. E. McQuade and S. J. Lippard, *Inorg. Chem.*, 2010, **49**, 7464; (d) Y. You, E. Tomat, K. Hwang, T. Atanasijevic, W. Nam, A. P. Jasanoff and S. J. Lippard, *Chem. Commun.*, 2010, **46**, 4139; (e) P. Du and S. J. Lippard, *Inorg. Chem.*, 2010, **49**, 10753.
- (a) V. Amendola, L. Fabbri and L. Mosca, *Chem. Soc. Rev.*, 2010, **39**, 3889; (b) V. Amendola, M. Boiocchi, B. Colasson, L. Fabbri, E. Monzani, M. J. Douton-Rodriguez and Cristina Spadini, *Inorg. Chem.*, 2008, **47**, 4808; (c) V. Amendola and L. Fabbri, *Chem. Commun.*, 2009, 513; (d) M. Vazquez, L. Fabbri, A. Taglietti, R. M. Pedrido, A. M. Gonzalez-Noya and M. R. Bermejo, *Angew. Chem., Int. Ed.*, 2004, **43**, 1962.
- (a) E. Arturoni, C. Bazzicalupi, A. Bencini, C. Caltagirone, A. Danesi, A. Garau, C. Giorgi, V. Lippolis and B. Valtancoli, *Inorg. Chem.*, 2008, **47**, 6551; (b) C. Bazzicalupi, A. Bencini, E. Faggi, A. Garau, C. Giorgi, V. Lippolis, A. Perra and B. Valtancoli, *Dalton Trans.*, 2006, 1409; (c) M. Mamelì, V. Lippolis, C. Caltagirone, J. Capelo, O. N. Faza and C. Lodeiro, *Inorg. Chem.*, 2010, **49**, 8276–8286.
- (a) G. Ambrosi, P. Dapporto, M. Formica, V. Fusi, L. Giorgi, A. Guerri, M. Micheloni, P. Paoli, R. Pontellini and P. Rossi, *Inorg. Chem.*, 2006, **45**, 304; (b) G. Ambrosi, M. Formica, V. Fusi, L. Giorgi, E. Macedi, M. Micheloni, P. Paoli and P. Rossi, *Inorg. Chem.*, 2009, **48**, 10424; (c) G. Ambrosi, M. Formica, V. Fusi, L. Giorgi, A. Guerri, E. Macedi, M.

- Micheloni, P. Paoli, R. Pontellini and P. Rossi, *Inorg. Chem.*, 2009, **48**, 5901; (d) G. Ambrosi, C. Battelli, M. Formica, V. Fusi, L. Giorgi, E. Macedi, M. Micheloni, R. Pontellini and Luca Prodi, *New J. Chem.*, 2009, **33**, 171.
- 30 (a) M. Alfonso, A. Espinosa, A. Tárraga and P. Molina, *Org. Lett.*, 2011, **13**, 2078; (b) M. Alfonso, A. Tárraga and P. Molina, *J. Org. Chem.*, 2011, **76**, 939; (c) F. Zapata, A. Caballero, A. Espinosa, A. Tárraga and P. Molina, *Org. Lett.*, 2008, **10**, 41; (d) F. Zapata, A. Caballero, A. Espinosa, A. Tárraga and P. Molina, *J. Org. Chem.*, 2009, **74**, 4787; (e) H. Xue, X.-J. Tang, L.-Z. Wu, L.-P. Zhang and C.-H. Tung, *J. Org. Chem.*, 2005, **70**, 9727; (f) D. Remeter, P. Blanchard, M. Allain, I. Grosu and J. Roncali, *J. Org. Chem.*, 2007, **72**, 5285; (g) A. Caballero, A. Espinosa, A. Tárraga and P. Molina, *J. Org. Chem.*, 2008, **73**, 5489.
- 31 (a) D. Saha, S. Das, D. Maity, S. Dutta and S. Baitalik, *Inorg. Chem.*, 2011, **50**, 46; (b) D. Saha, S. Das, C. Bhaumik, S. Dutta and S. Baitalik, *Inorg. Chem.*, 2010, **49**, 2334; (c) S. Das, D. Saha, C. Bhaumik, S. Dutta and S. Baitalik, *Dalton Trans.*, 2010, **39**, 4162; (d) C. Bhaumik, S. Das, D. Saha, S. Dutta and S. Baitalik, *Inorg. Chem.*, 2010, **49**, 5049.
- 32 Y. Miyamoto, A. Kikuchi, F. Iwahori and J. Abe, *J. Phys. Chem. A*, 2005, **109**, 10183.
- 33 (a) M. A. R. Meier and U. S. Schubert, *Chem. Commun.*, 2005, 4610; (b) B. G. G. Lohmeijer and U. S. Schubert, *Macromol. Chem. Phys.*, 2003, **204**, 1072; (c) R. Dobrawa, M. Lysetska, P. Ballester, M. Grüne and F. Würthner, *Macromolecules*, 2005, **38**, 1315; (d) U. S. Schubert and C. Eschbaumer, *Angew. Chem., Int. Ed.*, 2002, **41**, 2892.
- 34 (a) J.-P. Sauvage, J. P. Collin, J. C. Chambron, S. Guillerez, C. Coudret, V. Balzani, F. Barigelletti, L. De Cola and L. Flamigni, *Chem. Rev.*, 1994, **94**, 993; (b) E. Baranoff, J. P. Collin, L. Flamigni and J.-P. Sauvage, *Chem. Soc. Rev.*, 2004, **33**, 147; (c) E. C. Constable, *Chem. Soc. Rev.*, 2004, **33**, 373; (d) H. Hofmeier and U. S. Schubert, *Chem. Soc. Rev.*, 2004, **33**, 373; (e) E. A. Medlycott and G. S. Hanan, *Coord. Chem. Rev.*, 2006, **250**, 1763; (f) S. Baitalik, X. Wang and R. H. Schmehl, *J. Am. Chem. Soc.*, 2004, **126**, 16304; (g) X. Wang, A. Del Guerso, S. Baitalik, G. Simon, G. B. Shaw, L. X. Chen and R. H. Schmehl, *Photosynth. Res.*, 2006, **87**, 83.
- 35 (a) W. Goodall and J. A. G. Williams, *Chem. Commun.*, 2001, 2514; (b) M. Licini and J. A. G. Williams, *Chem. Commun.*, 1999, 1943; (c) W. Goodall and J. A. G. Williams, *J. Chem. Soc., Dalton Trans.*, 2000, 2893.
- 36 (a) F. Barigelletti, L. Flamigni, M. Guardigli, J.-P. Sauvage, J.-P. Collin and A. Sour, *Chem. Commun.*, 1996, 1329; (b) F. Barigelletti, L. Flamigni, G. Calogero, L. Hammarström, J.-P. Sauvage and J.-P. Collin, *Chem. Commun.*, 1996, 2334.
- 37 D. D. Perrin, W. L. Armarego and D. R. Perrin, *Purification of Laboratory Chemicals*, 2nd ed.; Pergamon, Oxford, U.K., 1980.
- 38 K. T. Pott, D. A. Usifer and H. D. Abruna, *J. Am. Chem. Soc.*, 1987, **109**, 3961.
- 39 F. H. Case and T. J. Kaspen, *J. Am. Chem. Soc.*, 1956, **78**, 5842.
- 40 W. Spahni and G. Calzaferri, *Helv. Chim. Acta*, 1984, **67**, 450.
- 41 E. C. Constable, M. D. Ward and S. Corr, *Inorg. Chim. Acta*, 1988, **141**, 201.
- 42 H.-J. Schneider and A. Yatsimirsky, *Principles and Methods in Supramolecular Chemistry*, John Wiley and Sons, London, 2000; p 142.
- 43 (a) K. Nakamaru, *Bull. Chem. Soc. Jpn.*, 1982, **55**, 1639 and references therein; (b) J. N. Demas and G. A. Crosby, *J. Am. Chem. Soc.*, 1971, **93**, 2841.
- 44 SAINT (version 6.02), SADABS (version 2.03), Bruker AXS Inc., Madison, Wisconsin, 2002.
- 45 G. M. Sheldrick, *SHELXL-97, Program for the Refinement of crystal Structures*, University of Göttingen, Göttingen, Germany, 1997.
- 46 *SHELXTL* (version 6.10), Bruker AXS Inc., Madison, Wisconsin, 2002.
- 47 A. L. Spek and PLATON, *J. Appl. Crystallogr.*, 2003, **36**, 7.
- 48 (a) P. P. Laine, F. Bedioui, F. Loiseau, C. Chiorboli and S. Campagna, *J. Am. Chem. Soc.*, 2006, **128**, 7510; (b) F. S. Han, M. Higuchi and D. G. Kurth, *Org. Lett.*, 2007, **9**, 559; (c) M. E. Padilla-Tosta, J. M. Lloris, R. Martínez-Mañez, A. Benito, J. Soto, T. Pardo, M. A. Miranda and M. Marcos, *Eur. J. Inorg. Chem.*, 2000, 741; (d) X.-Y. Wang, A. D. Guerso and R. H. Schmehl, *Chem. Commun.*, 2002, 2344.
- 49 (a) S. Leroy, S. Soujanya and F. Fages, *Tetrahedron Lett.*, 2001, **42**, 1665; (b) G. Albano, V. Balzani, E. C. Constable, M. Maestri and D. Smith, *Inorg. Chim. Acta*, 1998, **277**, 225; (c) D. Roberto, F. Tessore, R. Ugo, S. Bruni, A. Manfredi and S. Quici, *Chem. Commun.*, 2002, 846.
- 50 (a) Z. R. Grabowski and K. Rotkiewicz, *Chem. Rev.*, 2003, **103**, 3899; (b) R. M. Hermant, N. A. Bakker, T. Scherer, B. Krijnen and J. W. Verhoeven, *J. Am. Chem. Soc.*, 1990, **112**, 1214; (c) C. Reichardt, *Chem. Rev.*, 1994, **94**, 2319.
- 51 (a) J. R. Winker and N. Sutin, *Inorg. Chem.*, 1987, **26**, 220; (b) C. Creutz, M. Chou, T. L. Netzel, M. Okumura and N. Sutin, *J. Am. Chem. Soc.*, 1980, **102**, 1309; (c) M. A. Bergkamp, P. Guetlich, T. L. Netzel and N. Sutin, *J. Phys. Chem.*, 1983, **87**, 3877.
- 52 C. S. Wilcox, *Frontiers in Supramolecular Chemistry and Photochemistry*, VCH, Weinheim, Germany, 1991; pp 123-143.
- 53 (a) V. Balzani, N. Sabbatini and F. Scandola, *Chem. Rev.*, 1986, **86**, 319; (b) S. O. Kang, D. Powell, V. W. Day and K. Bowman-James, *Angew. Chem., Int. Ed.*, 2006, **45**, 7882; (c) T. Gunlaugasson, P. E. Kruger, P. Jensen, J. Tierney, H. D. P. Ali and G. M. Hussey, *J. Org. Chem.*, 2005, **70**, 10875; (d) D. E. Gomez, L. Fabbriizzi and M. Liccheli, *J. Org. Chem.*, 2005, **70**, 5717; (e) V. Amendola, D. Boiocchi, B. Colasson and L. Fabbriizzi, *Inorg. Chem.*, 2006, **45**, 6138; (f) S.-S. Sun, J. A. Anspach, A. J. Lees and P. Y. Zavalij, *Organometallics*, 2002, **21**, 685; (g) T.-P. Lin, C.-Y. Chen, Y.-S. Wen and S.-S. Sun, *Inorg. Chem.*, 2007, **46**, 9201; (h) C.-F. Chow, B. K. W. Chiu, M. H. W. Lam and W.-Y. Wong, *J. Am. Chem. Soc.*, 2003, **125**, 7802; (i) M. S. Han and D. H. Kim, *Angew. Chem., Int. Ed.*, 2002, **41**, 3809.
- 54 R. Shukla, T. Kida and B. D. Smith, *Org. Lett.*, 2000, **2**, 3099.
- 55 G. Tumcharern, T. Tuntulani, S. J. Coles, M. B. Hursthouse and J. D. Kilburn, *Org. Lett.*, 2003, **5**, 4971.